Cell Medicine, Vol. 5, pp. 29–42, 2013
Printed in the USA.

2155-1790/12 $90.00 + .00
DOI: http://dx.doi.org/10.3727/215517913X666468
www.cognizantcommunication.com

Phenotype and Stability of Neural Differentiation of Androgenetic Murine ES Cell-Derived Neural Progenitor Cells

Wanja Wolber,*[1] Ruhel Ahmad,†[1] Soon Won Choi,†[1,2] Sigrid Eckardt,‡ K. John McLaughlin,‡ Jessica Schmitt,† Christian Geis,§ Manfred Heckmann,¶ Anna-Leena Sirén,* and Albrecht M. Müller†

*Department of Neurosurgery, University of Würzburg, Würzburg, Germany
†Institute for Medical Radiation and Cell Research (MSZ) in the Center of Experimental and Molecular Medicine (ZEMM), University of Würzburg, Würzburg, Germany
‡Nationwide Children's Research Institute, Columbus, OH, USA
§Department of Neurology, University of Würzburg, Würzburg, Germany
¶Institute for Physiology, University of Würzburg, Würzburg, Germany

Uniparental zygotes with two paternal (androgenetic, AG) or two maternal genomes (gynogenetic, GG) cannot develop into viable offsprings but form blastocysts from which pluripotent embryonic stem (ES) cells can be derived. For most organs, it is unclear whether uniparental ES cells can give rise to stably expandable somatic stem cells that can repair injured tissues. Even if previous reports indicated that the capacity of AG ES cells to differentiate in vitro into pan-neural progenitor cells (pNPCs) and into cells expressing neural markers is similar to biparental [normal fertilized (N)] ES cells, their potential for functional neurogenesis is not known. Here we show that murine AG pNPCs give rise to neuron-like cells, which then generate sodium-driven action potentials while maintaining fidelity of imprinted gene expression. Neural engraftment after intracerebral transplantation was achieved only by late (22 days) AG and N pNPCs with in vitro low colony-forming cell (CFC) capacity. However, persisting CFC formation seen, in particular, in early (13 or 16 days) differentiation cultures of N and AG pNPCs correlated with a high incidence of trigerm layer teratomas. As AG ES cells display functional neurogenesis and in vivo stability similar to N ES cells, they represent a unique model system to study the roles of paternal and maternal genomes on neural development and on the development of imprinting-associated brain diseases.

Key words: Embryonic stem (ES) cell; Uniparental; Electrophysiology; Teratoma; Brain injury

INTRODUCTION

Pluripotent stem cells are invaluable tools for studying cell and tissue differentiation. They can be isolated from different sources including the embryonic inner cell mass (ICM), primordial germ cells, epiblast, and reprogrammed somatic cells (iPS cells) (14). Pluripotent stem cells can also be derived from the genetic information of paternal or maternal gametes exclusively. Uniparental embryos with two maternal genomes [gynogenetic (GG) or parthenogenetic (PG)] or two paternal genomes [androgenetic (AG)] have been experimentally generated in several mammalian species, including mouse [AG/GG (36,46) and PG (23)], long-tailed macaque fascicularis [PG (10)], and human [PG (30,35,43)]. While some vertebrate species such as lizards and snakes can reproduce successfully by parthenogenesis, mammalian uniparental embryos, although able to give rise to embryonic stem (ES) cells, do not develop into viable offspring due to cell autonomous defects as a result of unbalanced parent-of-origin-specific gene expression (39). Deregulated expression of imprinted genes, by either genetic or epigenetic alterations, can cause developmental abnormalities and cancer. In the brain, more than 1,300 transcripts are imprinted (1,15,24,50), implying that balanced expression

Received June 29, 2012; final acceptance May 29, 2013. Online prepub date: June 13, 2013.
[1]The authors provided equal contribution to this work.
[2]Present address: Adult Stem Cell Research Center, College of Veterinary Medicine, Seoul National University, Republic of Korea.
Address correspondence to Albrecht M. Müller, Institute for Medical Radiation and Cell Research (MSZ) in the Center of Experimental and Molecular Medicine (ZEMM), University of Würzburg, Zinklesweg 10, 97078 Würzburg, Germany. Tel: +(49) 931-201 45848; Fax: +(49) 931-201 45147; E-mail: albrecht.mueller@uni-wuerzburg.de *or* Anna-Leena Sirén, Department of Neurosurgery, University of Würzburg, Josef-Schneider Str. 11, 97080 Würzburg, Germany. Tel: +(49) 931-201 24579; Fax: +(49) 931-201 24140; E-mail: siren.a@nch.uni-wuerzburg.de

of imprinted genes is critical to brain development and function. Indeed, altered imprinting in the brain results in developmental and behavioral disorders (13,51). It is therefore not surprising that earlier analyses in a murine chimera model reported cell autonomous differences in the differentiation properties of AG and PG cells (29). Due to the severe phenotype of AG ES cells chimeras and due to the absence of primate and human AG ESCs (2,36,47), the developmental potential of AG ES cells has not been analyzed in detail. Our recent findings, however, indicated an equivalency of bi- and uniparental AG ES cells, as both normally fertilized (N) and AG ES cells underwent in vitro and in vivo development into hematopoietic and neural cell types including dopaminergic neurons (9,17,19).

To further address the tissue-specific differentiation potential for neural tissues, we determined the capacity of AG ES cells to undergo in vitro differentiation into functional neurons. Using a stereotactic transplantation paradigm, we assessed the safety and engraftment potential of AG ES-derived neural progenitor cells in vivo.

MATERIALS AND METHODS

ES Cell Culture

AG (AGA2, AGB6), N (wtB1) enhanced green fluorescent protein (eGFP) transgenic male murine ES cells used in this study have been previously described (17,20). V6.5 wild-type male murine ES cells were purchased from Open Biosystems, Thermo Scientific (St. Leon-Rot, Germany). AG and N ES cells were cultured on Mitomycin C-treated primary self-isolated murine embryonic fibroblasts (MEFs; Mitomycin-C from Sigma-Aldrich, Steinheim, Germany) in ESC growth medium, which consisted of Dulbecco's modified Eagle's medium (DMEM) (PAA Laboratories, Cölbe, Germany) supplemented with 15% ES cell-tested fetal calf serum (FCS) (PAA), leukemia inhibitory factor (LIF)-conditioned DMEM (PAA), 1% non-essential amino acids (PAA), penicillin/streptomycin (100 U/ml) (PAA), 2 mM L-glutamine (PAA), 1 mM sodium pyruvate (PAA), and 0.1 mM β-mercaptoethanol (Sigma-Aldrich, Taufkirchen, Germany), as previously described (17). ES cells used for in vitro differentiation and transplantation experiments were at passages 20–40.

Generation and Differentiation of pNPCs

ES cells were differentiated into neural lineages as described (6,25,40). For neural differentiation, MEFs were separated from ES cell cultures using differential adhesion. 1.5×10^6 ES cells were resuspended in 10 ml DMEM supplemented with 10% (v/v) FCS, 1% (v/v) non-essential amino acids, penicillin/streptomycin (100 U/ml), 2 mM L-glutamine, 1 mM sodium pyruvate, and 0.1 mM β-mercaptoethanol and plated on nonadherent Petri dishes (Greiner Bio One, Essen, Germany). After 5 days, embryoid bodies (EBs) were transferred to tissue culture plates (NUNC, Wiesbaden, Germany) and cultured in neural selection medium ITS/Fn consisting of DMEM/Ham's F-12 (PAA), penicillin/streptomycin (100 U/ml), 2 mM L-glutamine, human transferrin (50 g/ml) (Sigma-Aldrich), 30 nM sodium selenite (Sigma-Aldrich), insulin (5 g/ml) (Sigma-Aldrich), and fibronectin (2.5 μg/ml) (Sigma-Aldrich). After 4 days, cells were trypsinized (Sigma-Aldrich), triturated, and further cultivated on polyornithine- and laminin-coated dishes (Sigma-Aldrich) for 4 days in N3 medium (Gibco-Invitrogen, Karlsruhe, Germany) supplemented with 50 ng/ml fibroblast growth factor-2 (FGF2) (PeproTech, Hamburg, Germany) in DMEM/Ham's F-12. Pan-neural progenitor cells (pNPCs) were passaged every third day up to 22 days.

For induction of neuronal differentiation, day 16 pNPCs of AG and N origin were plated on poly-D-lysine (PDL, Sigma-Aldrich) coated 12-mm cover slips (Menzel, Braunschweig, Germany) in four-well plates (NUNC) at a density of 44,000 cells/cm² and grown in 500 μl of Neurobasal medium (Invitrogen, Karlsruhe, Germany) supplemented with 2 mM L-glutamine, penicillin/streptomycin (100 U/ml), and 2% B27 supplement (Invitrogen) for 7 days (D7) or 14 days (D14). Half of the medium (250 μl) was substituted with fresh medium every 48 h.

Immunofluorescence Staining in Cell Culture

Cells were washed twice with ice-cold phosphate-buffered saline (PBS, Sigma-Aldrich, pH 7.4), fixed in 4% paraformaldehyde-PBS (Sigma-Aldrich) for 15 min, permeabilized with 0.2% Triton-X (Sigma-Aldrich) in PBS for 10 min, and blocked for 30 min with 10% normal horse serum (NHS) in PBS (Jackson Immunoresearch, Hamburg, Germany). The cells were incubated in primary antibody solution (1% NHS in PBS with primary antibodies) for 60 min, rinsed three times in PBS, and incubated with the secondary antibody solution (1% NHS in PBS with secondary antibodies) for 60 min. Finally, the cells were rinsed three times in PBS and embedded in an anti-bleaching Mowiol reagent with 300 nM 4′,6-diamidino-2-phenylindole (DAPI, Sigma-Aldrich).

The following antibodies were used: mouse monoclonal anti-microtubule associated protein-2 (MAP-2; 1:200, Millipore, Schwalbach, Germany), mouse monoclonal anti-nestin (1:500, BD Pharmingen, Heidelberg, Germany), rabbit polyclonal anti-synapsin (1:500, Synaptic Systems, Göttingen, Germany), guinea pig polyclonal anti-Tau (1:500, Synaptic Systems), cyanine 3 (Cy3)-labeled goat anti-rabbit, Cy3-labeled goat anti-mouse, Dylight 596-labeled goat anti-guinea pig, Dylight 649-labeled goat anti-rabbit, Dylight 649-labeled goat anti-mouse (1:500, Jackson ImmunoResearch).

Image Acquisition, Image Processing

Cell culture samples and brain sections were photographed with a Leica LSM TCS SP5 confocal microscope (Leica, Wetzlar, Germany). Due to the three-dimensional distribution of cell processes, Z-stacks with a 0.1-µm interval were combined with the "Z-stack project" function of ImageJ (MBF "ImageJ for Microscopy"; NIH, Bethesda, MD, USA). The different color channels were merged with the "merge channel" function of Image J.

Whole-Cell Patch Clamp Analysis

Cells grown on glass coverslips in neuronal differentiation medium for 14 days were transferred into a recording chamber and continuously superfused with extracellular solution containing 125 mM NaCl, 25 mM $NaHCO_3$, 25 mM glucose, 2.5 mM KCl, 1.25 mM NaH_2PO_4, 2 mM $CaCl_2$, 2 mM $MgCl_2$ (purged by 95% CO_2/5% O_2; all from Sigma-Aldrich). The K^+ and Na^+ ion channel antagonists tetraethylammonium chloride (TEA, Sigma-Aldrich, 30 mM), or tetrodotoxin (TTX, Sigma-Aldrich, 1 µM), respectively, were added to the extracellular solution. All experiments were performed at room temperature using an EPC 10 double patch clamp amplifier and pulse software (HEKA, Lambrecht, Germany). Electrodes were pulled from thick-walled borosilicate glass and filled with intracellular solution (140 mM KCl, 10 mM HEPES, 10 mM EGTA, 2 mM Na_2ATP, 2 mM $MgCl_2$) and had a resistance between 3 and 4.5 MΩ. Cells were held in whole-cell configuration at –80 mV and were discarded if the series resistance was higher than 25 MΩ at the beginning of the measurements.

Analysis of Gene Expression Using Quantitative RT-PCR

Total RNA was isolated from cultured cells by using peqGOLD RNAPure (peqLab Biotechnologie, Göttingen, Germany). Prior to reverse transcription, RNA isolates were treated with DNase I (Ambion, Applied Biosystems, Foster City, CA, USA). RNAs were reverse-transcribed into cDNAs using Moloney Murine Leukemia Virus (M-MLV) reverse transcriptase (Invitrogen). Quantitative RT-PCR reactions were performed and quantified with a Rotor-GeneTM 3000 (Corbett Life Science, LTF Labortechnologie, Wasserburg, Germany) using ABsolute QPCR SYBR Green mixes (ABgene, Hamburg, Germany). Samples were further normalized to β-actin. The identity of PCR products was confirmed by melting curve analysis. The calculation of relative gene expressions in AG cells compared to N was performed using the $2^{-\Delta\Delta Ct}$ method. Primer sequences for real-time RT-PCR (60°C) were β-actin (forward/reverse): GAT ATC GCT GCG CTG GTC GTC/ACG CAG CTC ATT GTA GAA GGT GTG G; *delta-like 1 homolog* (*Dlk1*): TGT CAA TGG AGT CTG CAA GG/AGG GAG AAC CAT TGA TCA CG; *H19* [*imprinted maternally expressed transcript* (*non-protein coding*)]: CAT GTC TGG GCC TTT GAA/TTG GCT CCA GGA TGA TGT; *insulin-like growth factor 2* (*Igf2*): CTA AGA CTT GGA TCC CAG AAC C/GTT CTT CTC CTT GGG TTC TTT C; *insulin-like growth factor 2 receptor* (*Igf2r*): TAG TTG CAG CTC TTT GCA CG/ACA GCT CAA ACC TGA AGC G; *Impact*: ACG TTT CCC CAT TTT ACA AG/CTC TAC ATA TGA TTT TCT CTA C; *Nanog*: TCT TCC TGG TCC CCA CAG TTT/GCA AGA ATA GTT CTC GGG ATG AA; *Nestin*: CAG AGA GGC GCT GGA ACA GAG ATT/AGA CAT AGG TGG GAT GGG AGT GCT; *octamer binding transcription factor 4* (*Oct4*): CCG TGA AGT TGG AGA AGG TG/GAA GCG ACA GAT GGT GGT CT; *RNA exonuclease 1 homolog* (*Rex1*): GGC CAG TCC AGA ATA CCA GA/GAA CTC GCT TCC AGA ACC TG; *U2 small nuclear RNA auxiliary factor 2* (*U2af*): TAA GGC AGC ACC ACT TGG AC/CAT GGG AAG CCA GCT TAA AC; *ubiquitin protein ligase E3A* (*Ube3a*): CAC ATA TGA TGA AGC TAC GA/CAC ACT CCC TTC ATA TTC C; *maternally expressed zinc finger, imprinted 1* (*Zim1*): GAG AAG CCG TAC TGC TGT CA/CTT GCA CCG GTA CCT GGA GT. Expression analyses of *Musashi* and *cluster of differentiation 133* (*CD133*) genes by RT-PCR (60°C) were performed using QuantiTect Primer Assays (Qiagen, Düsseldorf, Germany).

Analysis of Gene Expression Using Semiquantitative RT-PCR

For analysis of genes expressed during neuronal differentiation total RNA was isolated from cultured cells (ESCs, d16 pNPCs and D7 pNPCs) by using TRIzol® (Invitrogen). Prior to cDNA generation, RNA isolates were treated with DNase I (Thermo Scientific). RNA was quantified spectrophotometrically and 1 µg taken for cDNA synthesis. M-MLV reverse transcriptase was used for reverse transcription of RNA into cDNA. Conditions for amplification with Taq Polymerase (HT Biotechnology, Cambridge, UK) were 94°C, 1 min; 60°C, 30 s; 72°C, 1 min (35 cycles). All reactions were performed on a peqStar 96 universal thermocycler (Peqlab GMBH, Erlangen, Germany) at 60°C. β-Actin was used as a control. Primers (Eurofins MWG Operon, Ebersberg, Germany) used for semiquantitative RT-PCR were β-actin (forward/reverse): GAT ATC GCT GCG CTG GTC GTC/CGC AGC TCA TTG TAG AAG GTG TGG; *ionotropic alpha-amino-3-hydroxy-5-methyl-4-isoxazole propionate glutamate receptor 1* (*AMPA1*): CAA GTT TTC CCG TTG ACA CAT C/CGG CTG TAT CCA AGA CTC TCT G; *calcium channel, voltage-dependent, L type, α 1C subunit* (*CaV1.2*): ATG AAA ACA CGA GGA TGT ACG TT/ACT GAC GGT AGA GAT GGT TGC; *γ-aminobutyric acid (GABA) A receptor, subunit α 1* ($Gaba_A\alpha_1$): GTC

ACC AGT TTC GGA CCA GT/TCA CGG TCA ACC TCA TGG TG.

Bisulfite Sequencing

Bisulfite sequencing of genomic DNA isolated from ESCs and pNPCs using the DNeasy Tissue Kit (Qiagen, Hilden, Germany) was performed as described (17,27). Analysis of sequences and diagram generation was performed using BiQ Analyzer (http://biq-analyzer.bioinf.mpi-sb.mpg.de) (4).

Colony-Forming Cell (CFC) Assay

To investigate the ability to form colonies, ES cells or pNPCs were cultured under ES cell culture conditions. After dissociation with trypsin, single cell suspensions were plated on 24-well MEF plates (NUNC) at cell densities of 200–500 for ES cells or 10^3–10^5 for pNPCs. Cells were cultured for 5 days in ESC growth medium as mentioned above. The number of ES cell-type alkaline phosphatase (AP)-active colonies was determined by staining of fixed cultures with the "leukocyte alkaline phosphatase" kit (Sigma-Aldrich) according to manufacturer's instructions. AP-positive ES cell-type colonies were counted and CFC frequencies of ES cell or pNPC cultures calculated based on the following morphological criteria: ES cell colonies on MEF feeders: round, clear boundary, strong AP staining (11); pNPC type colonies: not clear edged, less AP staining (Supplementary Fig. 1; http://www.strahlenkunde.uni-wuerzburg.de/ags/Suppl_material_Wolber_Ahmad_Choi_et_al.htm).

Stereotactic Transplantation

All experiments were approved by and conducted in accordance with the laws and regulations of the regulatory authorities for animal care and use in Lower Franconia, Germany. The lesions caused by cryogenic injury are circumscribed and reproducible in size, location, and pathophysiological processes (42). Four-week-old male C57BL6 mice (Charles River Wiga GmbH, Sulzfeld, Germany) were anesthetized with an intraperitoneal injection of ketamine (0.1 mg/g; Ketanest 10 mg/ml: Pfizer-Pharma, Berlin, Germany) and xylazine (0.005 mg/g; Rompun 2%: Bayer Health Care, Leverkusen, Germany). The parietal skull was exposed through a scalp incision, and a freezing lesion was placed on the right parietal cortex (coordinates from bregma: 1.5 mm posterior, 1.5 mm lateral). As previously described (42), the tip of a home-made cone-shaped copper cylinder with tip diameter of 2 mm was cooled with liquid nitrogen (−183°C) and stereotactically placed (stereotaxic apparatus: TSE Systems, Bad Homburg, Germany) in direct contact with the exposed parietal skull for 60 s. One week after setting of the lesion, mice were reanesthetized with ketamine-xylazine. Stereotactic injections into three sites surrounding the primary lesion were performed through a burr hole on three sites on the right brain hemisphere using the following coordinates from bregma: 1 mm, 2 mm, or 3 mm posterior; 1.5 mm lateral; 1.5 mm ventral from the surface of the dura. A 1-µl volume of the ES cell (1,000 cells/µl) or the pNPC (100,000 cells/µl) suspension in Hank's balanced salt solution (Sigma-Aldrich) was slowly injected into each site over 2 min by using a 5-µl Hamilton microsyringe (Hamilton, Reno, NV, USA), and the needle was gradually withdrawn over a period of 4 min. After transplantation, the scalp incision was sutured (5-0 Prolene, Ethicon, Johnson & Johnson, Livingston, UK), and the mice returned to their home cages. Recipients were monitored daily. Animals with any abnormalities were sacrificed immediately, and the brains were removed for histological analysis. All animals receiving grafts of ES cells, day 13 or day 16 pNPCs were sacrificed within 1 month posttransplant. Symptom-free animals with day 22 pNPC grafts were allowed to survive 3 months posttransplantation. At this point, mice were deeply anesthetized with ketamine–zylazine solution and a 20-ml volume of PBS followed with a 20-ml volume of 4% (w/v) paraformaldehyde (Applichem, Darmstadt, Germany) in PBS was perfused intracardially before removal of the brain.

Histology and Immunofluorescence Staining of Brain Cryosections

Brains were postfixed in 4% (w/v) paraformaldehyde (Applichem) in PBS for 1 day, cryoprotected in 16% (w/v) glucose (Applichem) in PBS for 2 days, embedded in TissueTek O.C.T. (Sakura Finetek, Heppenheim, Germany), frozen on dry ice, and stored at –80°C. Sagittal 10-µm-thick cryosections of the lesioned and transplanted right hemisphere were cut with a freezing microtome (Leica Biosystems, Nussloch, Germany) at –20°C. Every 10th section within the lesioned hemisphere was stained with hematoxylin–eosin (Sigma-Aldrich) for histological analysis of the lesion and engrafted donor material. Histological analysis was performed on hematoxylin–eosin stained sections. According to the 2007 guidelines of *Nature Biotechnology* teratomas were defined as tumors with differentiated tissue derived from more than one germ layer (12). Based on the presence of ectodermal, mesodermal, and endodermal differentiation, tumors were classified as teratomas with three germ layers (3GL). These teratomas were large and consisted of differentiated mesoderm (skeletal muscle, cartilage), ectoderm (neuroectoderm, keratinocytes, or ectodermal cavities), and endoderm (ciliated epithelium). Teratomas with two germ layers (2GL) were smaller and consisted of ectodermal and mesodermal derivatives. Additionally observed tissue clusters consisting of solely neuroectoderm were classified as neuroectoderm. To assess the survival and

differentiation of donor cells in transplanted brains, the engraftment of eGFP-labeled cells was assessed by immunohistochemical staining using a chicken polyclonal anti-eGFP (1:1,000, Abcam, Cambridge, UK), primary antibody, and a Cy2-labeled sheep anti-chicken (1:200, Abcam) secondary antibody.

Differentiated donor cells, neuroectodermal proliferation, 2GL and 3GL teratomas were assessed by immunohistochemical staining. Cryosections were dried for 30 min at room temperature, boiled in 10 mM sodium citrate buffer pH 6 (Sigma-Aldrich) in a microwave, and cooled down for 30 min at room temperature. Citrate buffer was replaced with H_2O, and slides were washed three times in PBS. After a 2-h incubation with PBS containing 5% NGS (normal goat serum, Jackson Immunoresearch) and 0.1% Triton-X, slides were incubated with the primary antibodies in 5% NGS-PBS over night at 4°C. On the next day, slides were washed three times in PBS and incubated for 1 h with the secondary antibodies in 5% NGS-PBS. The slides were rinsed three times in PBS and embedded in an antibleaching Mowiol reagent with 300 nM DAPI. The following primary antibodies were used: rabbit polyclonal anti-cleaved caspase-3 (1:200, Abcam), mouse monoclonal anti-proliferating cell nuclear antigen (PCNA; 1:1,000, BD Pharmingen), mouse monoclonal anti-stage specific embryonic antigen 1 (SSEA-1; 1:200, BioLegend, Aachen Germany), rabbit polyclonal anti-paired box 6 (Pax6; 1:200, Millipore), goat polyclonal anti-vimentin (1:200, Sigma-Aldrich), rabbit polyclonal, anti-calretinin (1:500, Synaptic Systems, Göttingen, Germany), and mouse monoclonal anti-NeuN (1:500, Millipore, Temecula, CA, USA). Secondary antibodies were Cy3-labeled goat anti-rabbit, Cy3-labeled goat anti-mouse, and Cy3-labeled rabbit anti-goat (1:500, Jackson ImmunoResearch).

Statistical Analysis

Results are presented as mean ± SD. Values of $p < 0.05$ were considered statistically significant. Statistical significance of the data was assessed by Student's two-tailed test for independent samples or with Mann–Whitney *U*-test for not normally distributed data. Correlation of in vitro pluripotency with teratoma formation were calculated using Pearson's test and the teratoma frequencies by Fischer exact probability test.

RESULTS

In Vitro Neural Potential of AG ES Cells

To assess their neural in vitro differentiation potential, AG ES cells were subjected to a multistep differentiation protocol that induces differentiation of ES cells into pan-neural progenitor cells (pNPCs) by formation of floating EBs, followed by EB attachment and pNPC formation (Fig. 1A, B). >95% of AG and N pNPCs stained positive for nestin, an intermediate filament that is expressed predominantly in neural stem/progenitor cells as well as endothelial cells (34). Both normal (N, derived from fertilized embryos) and AG ES cell-derived pNPCs lost expression of key pluripotency genes such as *Oct4*, *Nanog*, and *Rex1* after neural differentiation (Fig. 1C). In parallel, following neural induction, differentiated cells from ES cell cultures initiated the expression of neural genes such as the neural stem cell marker *Prominin-1/CD133*, the neural cell fate regulator *Musashi* and *Nestin* (Fig. 1C). Overall, expression analysis of selected pluripotency and neural genes revealed no differences between AG and N pNPC cultures. Day 22 AG-derived pNPC cultures maintained parent of origin-specific expression of several imprinted genes involved in brain development. Genes expressed from the paternal allele, including *Igf2* (insulin-like growth factor 2) and *Dlk1* (protein delta homolog 1), *Impact* and *U2af* (U2 auxiliary factor) were upregulated, while maternally expressed genes such as *Igf2r* (insulin-like growth factor 2 receptor), *H19* (long coding RNA), *Ube3a* (ubiquitin-protein ligase E3A), and *Zim1* (zinc finger imprinted 1) were silenced (Fig. 1D).

Allele-specific gene expression entails differentially methylated regions that carry parental allele-specific methylation profiles. Therefore, we analyzed methylation of CpG islands of two imprinting regulatory regions: *Igf2r's* differentially methylated region 2 (DMR2) and the intergenic differentially methylated region (IG-DMR) of *Dlk1*. The *Igf2r* gene is maternally expressed and the DMR2 of *Igf2r*, an intronic 3-kb CpG island, is maternally methylated (3). Bisulfite-sequencing analysis showed that CpG islands in DMR2 of *Igf2r* in AG pNPCs were predominantly not methylated, consistent with the maintenance of parent-of-origin-specific marks (Fig. 1E). Imprinting of the atypical NOTCH ligand *Dlk1* is controlled by an IG-DMR positioned between *Dlk1* and the adjacent gene *maternally expressed 3 (non-protein coding)* (*Gtl2*) (48). The paternally inherited copy is expressed. Consistent with a paternal origin, AG pNPCs show high-level *Dlk1* expression and a methylated IG-DMR (Fig. 1E).

AG ES cell-derived pNPCs were subject to neural differentiation conditions for up to 14 days, followed by analysis for neural markers, to investigate their differentiation potential. Costaining with the dendritic marker MAP-2 and the axonal marker Tau showed that cells with neuron-like morphology in day 14 (D14) differentiation cultures express markers of postmitotic neurons (MAP-2^+ AG cells: 28 ± 10%; MAP-2^+ N cells: 30 ± 11%, $n = 3$) (Fig. 2A). Presynaptic synapsin-1-positive dots could also be localized in the vicinity of dendritic processes expressing MAP-2. Expression of ligand-gated excitatory (*AMPA1*) and inhibitory ($Gaba_A\alpha 1$) receptors and the voltage-gated L-type calcium channel (*CaV 1.2* subunit) in AG and N pNPCs and differentiated cultures at day 7 (D7) further demonstrated the neuronal fate (Fig. 2B).

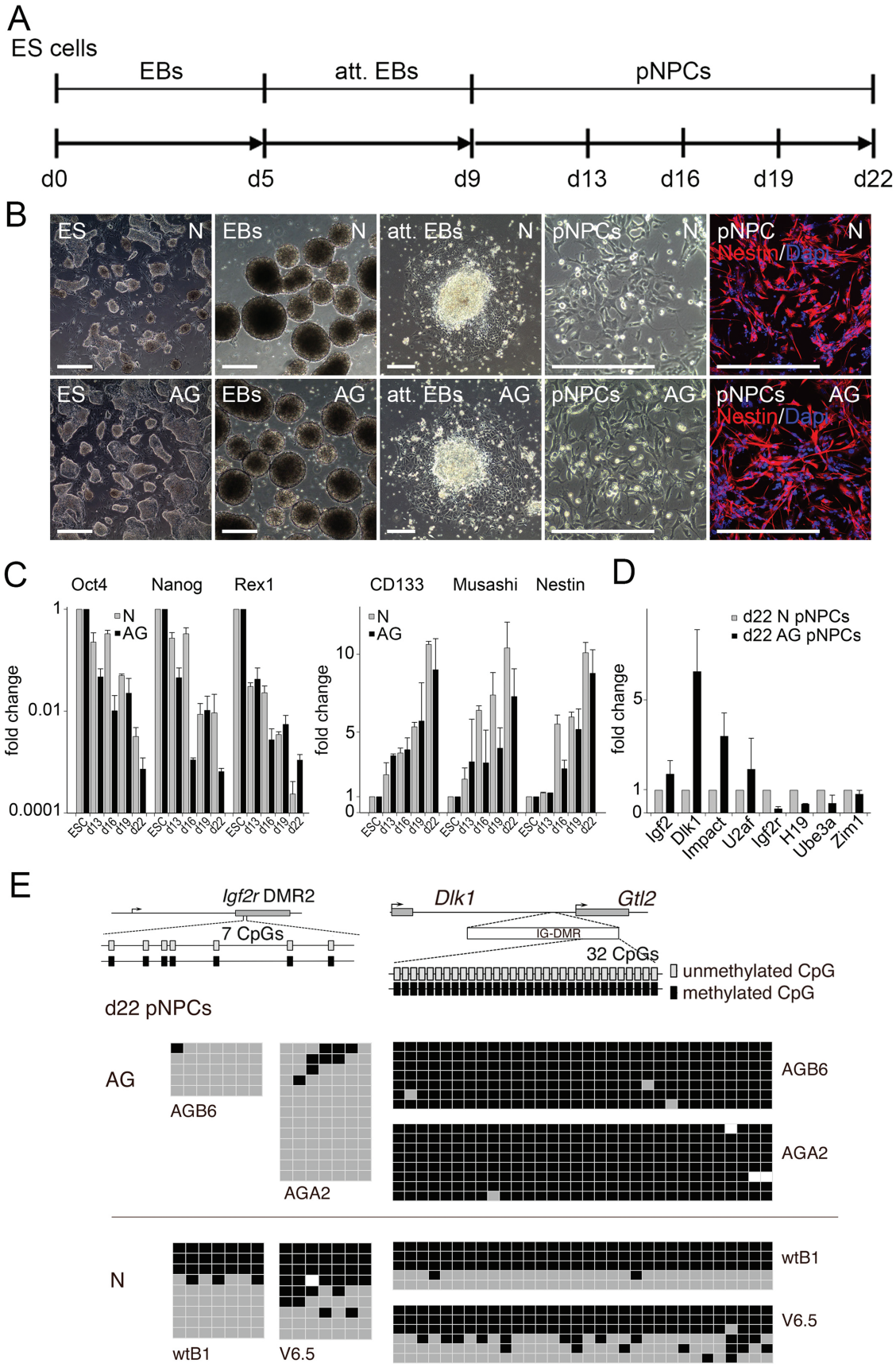
A
ES cells
EBs
att. EBs
pNPCs
d0
d5
d9
d13
d16
d19
d22
B
ES N
EBs N
att. EBs N
pNPCs N
pNPC N
Nestin/Dapi
ES AG
EBs AG
att. EBs AG
pNPCs AG
pNPCs AG
Nestin/Dapi
C
Oct4
Nanog
Rex1
CD133
Musashi
Nestin
N
AG
fold change
1
0.01
0.0001
10
5
1
0
ESC
d13
d16
d19
d22
D
d22 N pNPCs
d22 AG pNPCs
fold change
5
1
0
Igf2
Dlk1
Impact
U2af
Igf2r
H19
Ube3a
Zim1
E
Igf2r DMR2
7 CpGs
Dlk1
Gtl2
IG-DMR
32 CpGs
unmethylated CpG
methylated CpG
d22 pNPCs
AG
AGB6
AGA2
AGB6
AGA2
N
wtB1
V6.5
wtB1
V6.5

Electrophysiological Properties of AG ES-Derived Neurons

To explore whether AG similar to N pNPC-derived neuron-like cells develop functional membrane properties, cells with a neuron-like morphology were analyzed in whole-cell patch clamp recordings (Fig. 3). In current clamp (CC) mode, depolarizing step current injections (–50 pA to +130 pA, step size 20 pA) over a 500-ms time period elicited action potentials with a frequency of up to 20 Hz in all N- ($n=11$) and AG- ($n=12$) derived cells (Fig. 3A). In voltage clamp (VC) mode, action potentials were induced via stepwise cell depolarization (–80 mV to +55 mV, step size 15 mV) and corresponding voltage-gated Na^+ and K^+ channel currents were measured in both N- and AG-derived cells (Fig. 3B). When maximum in- and outward currents for each stimulating voltage were plotted against the stimulation voltage, AG- and N-derived neurons showed typical neuronal current patterns and similar current/voltage curves (Fig. 3C). The specificity of inward Na^+ ion and outward K^+ ion currents was verified by selective pharmacological blockers of sodium (tetrodotoxin) and potassium (tetraethylammonium) channels (Fig. 3E). The resting membrane potential of N and AG neurons at day 7 of in vitro pNPC differentiation ranged from –35 to –70 mV (N: –45 mV, 30 mV (median, range); AG: –41 mV, 15 mV). Other membrane properties such as cell capacity (N: 13 pF, 10.5 pF (median, range); AG: 8.8 pF, 7.4 pF) and inducible action potentials (Fig. 3D) were also similar between N and AG neurons and comparable to membrane properties reported in neuronal cells directly reprogrammed from fibroblasts (49). Together this indicates that AG pNPCs do not differ from N pNPCs in their potential to generate functional neuron-like cells in cell culture.

In Vitro ES-Like Colony Formation of AG-Derived pNPCs

To evaluate whether cells capable of forming ES cell-type colonies are still present in differentiating pNPC cultures, single cell suspensions of days 13–22 pNPCs were exposed to ES culture conditions. As shown in Figure 4A and in Supplementary Figure 1 intensively alkaline phosphatase-positive (AP^+) ES cell-type colonies were seen with undifferentiated ES cells. The colony formation decreased with increasing time of in vitro differentiation similarly in N and AG cultures. We observed, however, that the kinetics of loss of colony formation varied between cell lines.

In Vivo Tumor Formation of AG-Derived pNPCs

To evaluate the capacity of AG ES cell-derived pNPCs to engraft in vivo and to assess potential tumor formation, we injected single cell suspensions of AG pNPCs at various stages of in vitro differentiation as well as undifferentiated AG ES cells into the border zone of a cortical cryolesion. N ES cells and pNPCs were injected as controls. Highly reproducible lesions were induced by freezing through the skull bone with a liquid nitrogen-cooled copper cone (42). To avoid excessive loss of the transplanted cells due to acute postinjury inflammation (42), stereotactic transplantations were performed 1 week after lesion induction. Histological analysis of macroscopically normal brains of day 22 transplant recipients revealed small neuroectodermal cell clusters in 1 brain of 16 (1/16) AG and 2/21 N pNPC recipients. Small teratomas consisting of ecto- and mesodermal two germ layer components (teratoma 2GL) were found in 4 brains of 16 (4/16) AG and 3/21 N pNPC recipients (Fig. 4, Supplementary Fig. 2:

FACING PAGE

Figure 1. Neural in vitro differentiation of AG ES cells. (A) Time-scale diagram (days) for embryonic stem (ES) cell-derived in vitro neurogenesis via embryoid body (EB) formation, attached embryoid bodies (att. EBs), and pan-neural progenitor cells (pNPCs). (B) Phase contrast images of corresponding stages of in vitro neural differentiation and of immunostainings of day 13 pNPCs with a Nestin-specific antibody. Scale bars: 0.5 mm (ES) and 0.25 mm (EBs, att. EBs, and pNPCs). (C) Analysis of expression of pluripotency and neural progenitor genes in androgenetic (AG) and normal (N) cells during neural differentiation by quantitative RT-PCR. ESC, ES cells; d13, d16, d19, d22, ES cells differentiated for 13–22 days; Oct4, octamer binding transcription factor 4; Rex1, RNA exonuclease 1 homolog; CD133, cluster of differentiation 133. The relative expression represents the fold change of gene expression in AG and N cells. Fold change was calculated by the $2^{-\Delta\Delta Ct}$ method. Expression levels in AG and N ES cells were set to 1. $n=3$. (D) Relative expression levels of imprinted genes in day 22 AG pNPCs determined by real-time RT-PCR and calculated using the $2^{-\Delta\Delta Ct}$ method. Igf2, insulin-like growth factor 2; Dlk1, delta-like 1 homolog; U2af, U2 small nuclear RNA auxiliary factor 2; Impact; Igf2r, insulin-like growth factor 2 receptor; H19, imprinted maternally expressed transcript (non-protein coding); Ube3a, ubiquitin protein ligase E3A; Zim1, maternally expressed zinc finger, imprinted 1. Expression in N d22 pNPCs was set to 1. $n=3$. (E) Methylation status of the differentially methylated region 2 (DMR2) of the *Igf2r* gene and the intergenic differentially methylated region (IG-DMR) of the delta-like 1 homolog-maternally expressed 3 (non-protein coding) (*Dlk1-Gtl2*) domain in AG and N ESC-derived day 22 pNPCs. The methylation status of both DMRs is established during gametogenesis: the *Igf2r* DMR2 becomes methylated in the female germline, and the *Dlk1-Gtl2* IG-DMR methylated in male gametes. Consistent with paternal-only origin, AG ESC derived pNPCs (AGB6, AGA2) lack methylation at the *Igf2r* DMR2 (left) but maintain a fully methylated *Dlk1-Gtl2* IG-DMR (right). N ESC-derived pNPCs (wtB1, V6.5) contain methylated and unmethylated alleles of both DMRs. Each row represents a separate DNA molecule (clone).

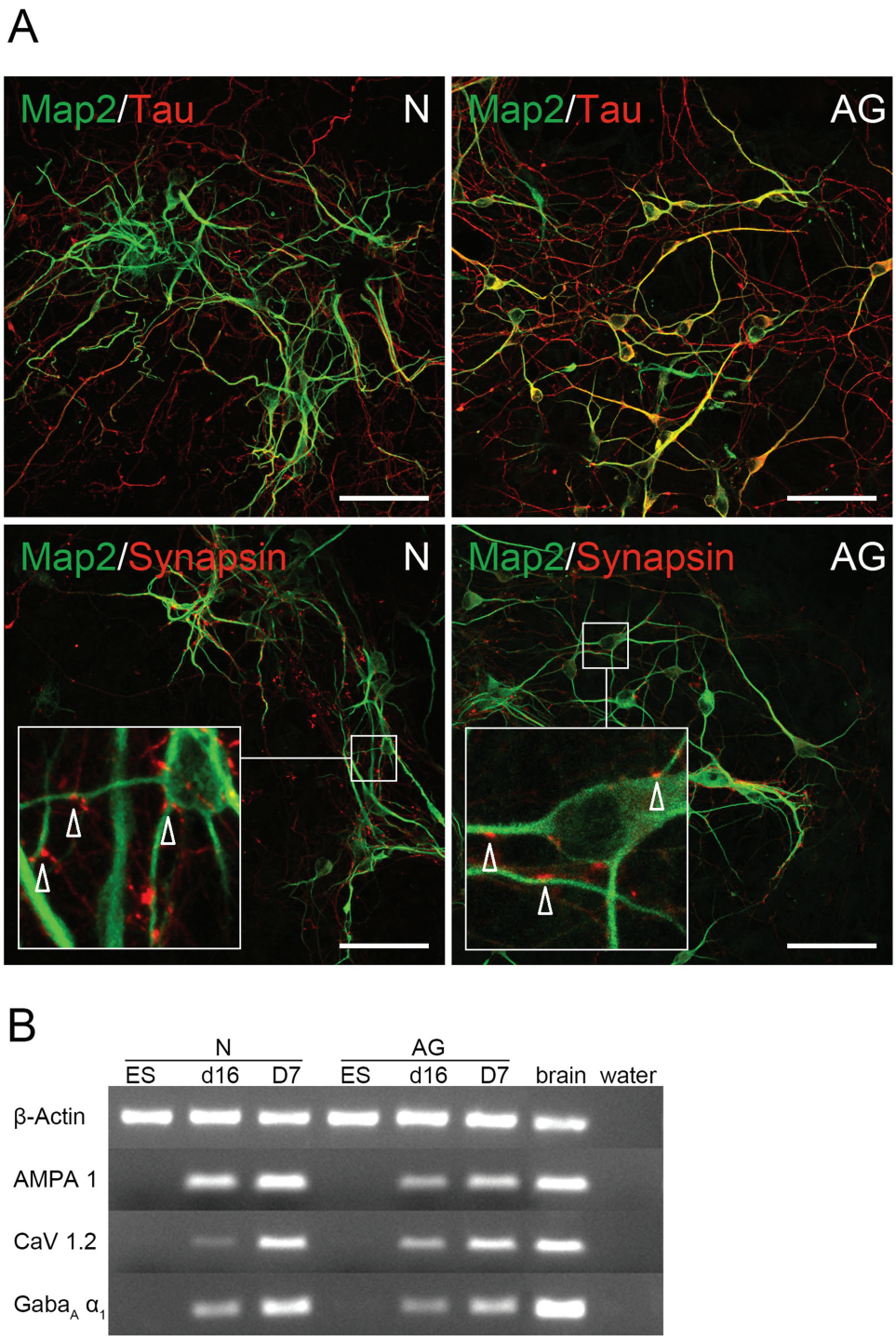

Figure 2. Immunophenotyping of AG ES cell-derived neurons. (A) Representative images of three biological replicates depicting neuronal marker expression in AG (right) and N (left) pNPC-derived cells after 14 days of differentiation. Scale bars: 50 µm. Upper row, visualization of microtubule associated protein 2 (MAP-2)$^+$ dendritic (green) and Tau$^+$ axonal (red) processes. Lower row, colocalization of synapsin-1$^+$ presynaptic dots (red) on MAP-2$^+$ dendritic processes (green). Arrows in the inset indicate synapsin-1$^+$ areas. (B) Analysis of expression of ligand and voltage gated channels in N and AG cells during neural differentiation by RT-PCR. ES, undifferentiated ES cells; d16, pNPCs after 16 days of differentiation, D7, d16 pNPCs after additional 7 days of neural differentiation ($n=6$); *AMPA1*, ionotropic alpha-amino-3-hydroxy-5-methyl-4-isoxazole propionate glutamate receptor 1; *CaV1.2*, calcium channel, voltage-dependent, L type, α 1C subunit; *Gaba$_A$α1*, gamma-aminobutyric acid (GABA) A receptor, subunit α 1.

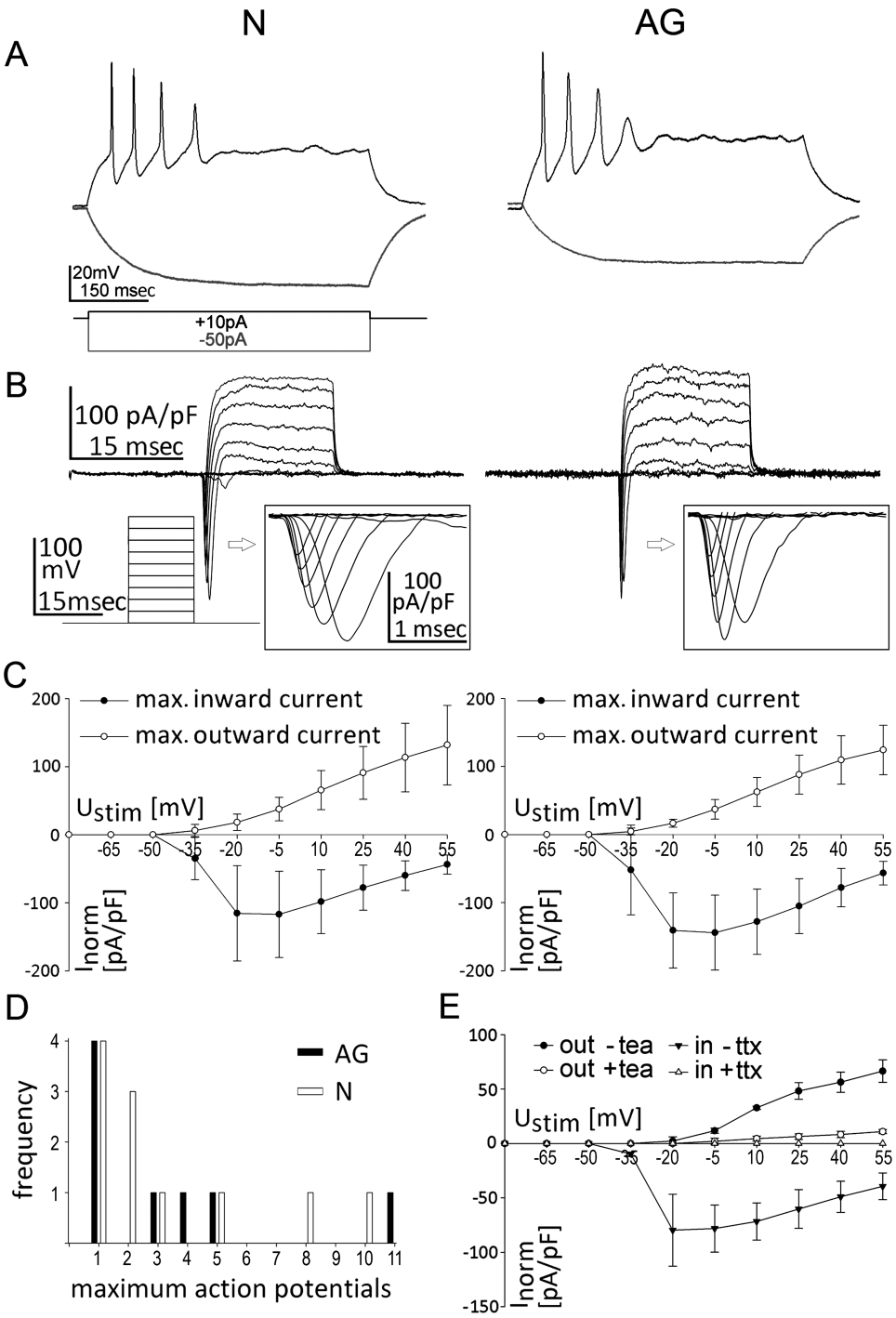

Figure 3. Electrophysiological properties of AG neurons. (A) Representative traces of membrane potential responding to step depolarization by current injection (depolarizations, black lines; hyperpolarizations, gray lines). Current injections (–50 pA, +10 pA) into AG and N pNPC-derived neurons in current clamp (CC)-mode. (B) Representative traces of whole-cell currents in voltage clamp mode responding to step depolarization by current injection. Inserts show sodium currents. Stimulation via stepwise increase of membrane potential (–80 mV to +55 mV, step size 15 mV) in VC-mode. (C) Current (I)/voltage (V) curves of voltage clamp (VC)-stimulation. Stimulation potential (mV) is plotted against the highest and the lowest measured current [current is normalized to cell size (pA/pF)]. Data represent mean ± SD, $n = 3$. (D) Frequency of maximum action potentials that could be induced in current clamp (CC)-mode. Action potentials were induced by current injection (+10 pA) into AG (black column) and N cells (white column). (E) I/V curves of VC-stimulation in AG-derived neurons before and after treatment with tea (tetraethylamonium, potassium channel blocker) or ttx (tetrodotoxin, sodium channel blocker). Stimulation potential (mV) is plotted against the highest and the lowest measured current [current was normalized to cell size (pA/pF)]. Data are mean ± SD, $n = 3$.

A

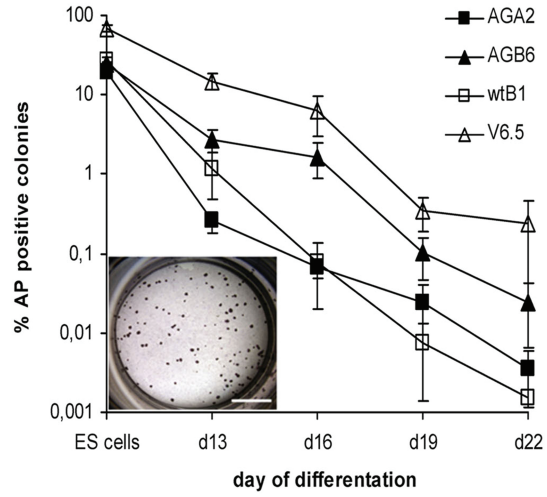

B

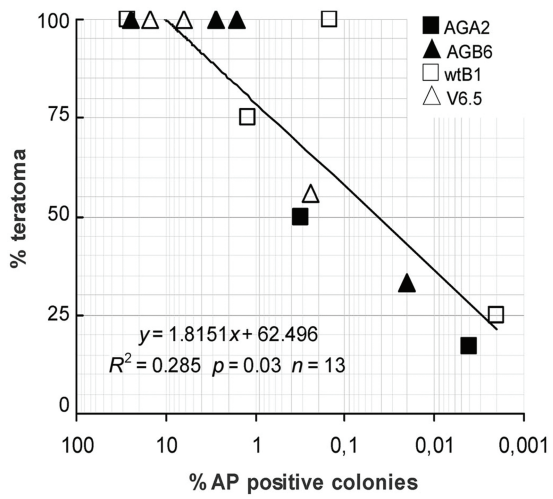

C

differentiation state	cell line	analysis after 1 month	analysis after 3 months
ES cells	wtB1	■■	
	AGB6	■	
d13 pNPCs	wtB1	■■■□	
	V6.5	■	
	AGB6	■	
	AGA2	■□	
d16 pNPCs	wtB1	■■■■	
	V6.5	■■	
	AGB6	■■■■■■	
d22 pNPCs	wtB1	■□□	■■□□□□□□□
	V6.5	■▒▒	■▒▒□□□
	AGB6	□□□	■▒▒▒▒□□□□
	AGA2		▒▒□□□

■ = teratoma-3GL ▒ = teratoma-2GL ▒ = neuroectoderm □ = tumor free

D

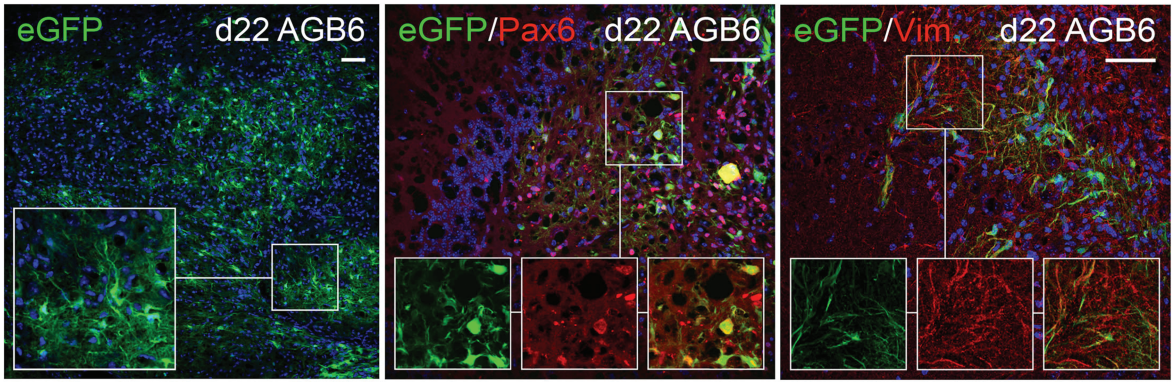

http://www.strahlenkunde.uni-wuerzburg.de/ags/Suppl_material_Wolber_Ahmad_Choi_et_al.htm). Smaller teratomas with two germ layers or neuroectodermal cell clusters were only found following transplantation of day 22 pNPCs. Not surprisingly, transplantation of undifferentiated AG or N ES cells resulted in the formation of macroscopically visible solid teratomas in the transplanted brain tissue of all mice within 4 weeks. Similarly, most recipients of day 13 or day 16 pNPCs developed highly differentiated solitary teratomas consisting of all three germ layers that grew confined to the injection site, regardless of N or AG origin of the transplant.

Comparison of the in vitro CFC frequencies of the transplanted cells with the occurrence of teratomas after transplantation revealed a linear correlation between the in vitro colony-forming capacity and teratoma formation in vivo (Fig. 4B). Qualitatively, AG- and N-derived teratomas had similar appearance and morphology.

To further characterize the small clusters immunostainings for ES cell markers, markers for cell proliferation and apoptosis were performed. As shown in Supplementary Figure 3, small clusters stained positive for cleaved caspase-3 and weakly positive for PCNA indicating dying as well as proliferating cells. In contrast to cells in 3GL teratomas that stained positive for PCNA and SSEA1 and which were weakly positive for cleaved caspase-3, cells in small clusters had lost expression of the stem cell/progenitor cell marker SSEA1 (8).

Neural/Glial Engraftment of AG-Derived pNPCs

Finally, we assessed the neural engraftment of AG ES cell-derived pNPCs 3 months posttransplantation into cryolesioned brains; 7/14 AG recipients and 10/15 N recipients that had received day 22 pNPC transplants did not show tumor formation (Fig. 4C). In these animals, donor cells were found close to the injection site. eGFP$^+$ ES cell derivatives exhibited various shapes and stained positive for early neuronal and glial markers (Fig. 4D). Quantification of eGFP$^+$ cells in brain sections revealed no difference between AG and N transplants in respect to total number of transplant-derived cells or number of transplant derivatives that had acquired neural morphology (eGFP$^+$ donor cells with neural morphology: AGA2 recipients: 57 and 91 cells/mm^2, $n=2$; AGB6 recipients: 124 ± 63 cells/mm^2, $n=4$; wtB1 recipients 170 ± 85 cells/mm^2, $n=3$, mean $\pm$ standard deviation).

The eGFP$^+$ cells in brain sections stained positive for the early markers (vimentin, Pax6) (Fig. 4D). Nevertheless, the engrafted eGFP$^+$ ES cell-derived pNPCs did not form mature neurons after 3 months. Staining for late neural markers (calretinin, NeuN, MAP-2, synapsin-1) was restricted to the recipient's neuronal tissue (data not shown).

DISCUSSION

Here, we report that both AG and N ES-derived neural progenitor cells successfully undergo neural in vitro differentiation and engraft in a brain injury model in vivo, with similar tumorgenicity of AG and N cells.

Dynamic developmental stage-regulated and cell type-specific imprinting of brain gene expression has been suggested to be important for normal brain development (21). In addition to previous studies revealing biased contribution of AG and PG cells in the brains of fetal stage chimeras, a recent high-resolution analysis of parent-of-origin-specific gene expression in the murine brain revealed a preferential maternal contribution to gene expression in the developing brain and a major paternal contribution in the adult brain (24). Thus, functional differences of the parental genomes during brain development and in the adult brain may limit the neural differentiation capacity of AG ES cells. Here, we observed that AG ES cells, despite a missing maternal-specific genome, can undergo neuronal in vitro development and in vivo engraftment similarly to N ES cells. These results are consistent with our previous studies demonstrating unrestricted distribution of AG ES cell derivatives to neuronal and glial cell lineages in blastocyst injection chimeras (9,17). The observation that AG ES cell-derived neural progenitor/stem cells survive and their further differentiation is possible in the absence of a maternal genome indicates that AG ES cells may have different differentiation potential compared to AG ICM

FACING PAGE

Figure 4. Decreased ES colony and teratoma formation upon prolonged differentiation of AG ES cell-derived pNPCs and neural/glial engraftment of day 22 pNPCs. (A) Frequencies of alkaline phosphatase$^+$ (AP$^+$) colony formation after culture of undifferentiated ES cells or dissociated day 13 to day 22 pNPCs in ES cell culture conditions. Inset shows the AP staining of day 13 pNPC-derived colonies. AG lines, filled symbols; N lines, empty symbols. Scale bar: 0.5 mm. (B) Pearson's correlation analysis of in vitro AP$^+$ colony and in vivo teratoma formation of AG and N ES cells and of day 13, 16 and 22 pNPCs. (C) Teratoma formation in recipients after transplantation of undifferentiated N and AG ES cells and of N and AG ES cell-derived pNPCs at different stages of in vitro differentiation. Boxes represent the histological outcome for each recipient at time of sacrifice. Teratoma 3GL, 3 germ layers; teratoma 2GL, 2 germ layers. Recipients were monitored for tumor formation up to 3 months when they were sacrificed and analyzed. (D) Representative images showing neural engraftment upon transplantation of day 22 AG pNPCs. Recipients were analyzed 3 months after transplantation. Immunohistochemical staining and *Z*-stack analysis of brain samples show enhanced green fluorescent protein (eGFP) positive donor cells (left) and cells with coexpression of eGFP and neural markers paired box 6 (Pax6; middle) and vimentin (right). Scale bars: 50 μm.

cells. Furthermore, neural progenitor formation and further differentiation can occur in the presence of abnormal levels of imprinted genes. Several possibilities exist to explain the apparent contradiction between these results and the relevance of imprinted gene expression in the brain. Parent of origin-specific transcriptional biases may contribute to the complex social behavior of animals and humans, but not or much less to the characteristics and behavior of cells in vitro (28). Likewise, it is conceivable that AG neural progenitor cells express functional differences that are not measured by our analyses but they could be important for the formation of synapses and other cell–cell interactions. Finally, the normal (biparental) brain environment may guide the fate and differentiation of uniparental donor cells. Indeed, recent studies on transplanted neural stem/progenitor cells indicated a multitude of environment-dependent influences on engrafted cells in their new environment (33).

Early proliferation and neuronal differentiation followed by neuronal maturation and functional activity of the grafted hES- and hiPS-derived progenitor cells is known to take place in the first weeks after transplantation in rat models of stroke (7,41). These early events have been suggested to improve recovery by inducing trophic effects on the host brain whereas axonal sprouting and synaptic inputs between the grafted cells and host brain may lead to functional tissue reconstruction much later during the stroke recovery (7,32,41). In the present study, both AG and N pNPCs survived and expressed early differentiation markers for neurons and glia 3 months after intracerebral transplantation. However, even if the cells exhibited neuron-like activity, expressed ligand and voltage-gated ion channels and were able to generate action potentials in vitro, we could not detect synaptic integration of the transplanted cells in the recipient's brain. It is conceivable that the damaged brain environment negatively influenced neuronal differentiation of the engrafted cells in vivo, and therefore, the 3-month time point was too early to detect such a functional maturation. Mouse ES cell-derived pNPCs survive and show long-term engraftment and integration 9 months after intracranial transplantation in an intact brain while no cells survived in an injured cortex after stroke (18). Similar results were recently reported after transplantation of mouse neural stem cells into an injured mouse spinal cord (33). In this latter study extraction of the engrafted cells was only possible within the first days after grafting as most cells in the injured neural tissue did not survive. In agreement with these findings, we were able to detect only few engrafted cells in the recipient brains 3 months after transplantation. Therefore, a further analysis of their detailed phenotype and differentiation profile by extraction and purification was not possible. A functional integration of transplanted hES cells even into fetal or newborn healthy mouse brain is detected only at earliest 4–18 months after intracerebral transplantation (31,38), and recent studies provide evidence for direct inhibitory influences of the damaged neuronal tissue on neuronal differentiation and maturation of engrafted neural stem cells (32,33).

Concerns have been raised over the safety of pluripotent ES-derived tissue stem cells including ES-derived neural stem cells whether there is the potential of tumor development upon stem cell transplantation (22). Tumorigenicity seems particularly critical for AG ES cells. Earlier studies reported that in vivo overexpression of the growth factor *Igf2* causes a perturbation of mesoderm formation and a hyperplasia of heart cell types (37). In AG mouse embryonic fibroblasts, increased *Igf2* expression stimulates proliferation that results in a rapid conversion of AG MEFs to malignancy with tumor formation of short latency (26). In AG pNPCs, we observed elevated levels of several paternally expressed genes, including *Igf2*, and reduced expression of the maternally expressed *Igf2r*. Yet, both N and AG-derived pNPCs formed benign teratomas after transplantation into the lesioned cortical tissue of mice, similar to the teratoma formation observed after intracerebral transplantation of biparental murine ES-derived pNPCs into rodent models of brain injury (5,16,44,45). Evidence for malignant transformation and development of teratocarcinomas was not seen in our material.

We observed a linear correlation between in vitro colony forming activity and teratoma formation for both AG and N pNPC cell cultures. Whereas the majority of recipients transplanted with undifferentiated or days 13–19 pNPCs developed a 3GL teratoma in the grafting site, recipients of day 22 pNPCs showed 3GL teratoma formation only in 1 brain of 17 (1/17) AG and 5/21 N pNPC recipients. This suggests that long-term in vitro differentiation reduces the proliferative and pluripotent potential of ES cell derivatives and the risk of tumor formation. This is in line with previously reported observations (16). Measurements of colony-forming activity could be used to predict safety at least in respect to teratoma formation to avoid the uncontrolled growth of ectopic tissue that compress and potentially damage host brain parenchyma.

In contrast to undifferentiated AG ES cells and early differentiation AG pNPCs that all led to formation of large differentiated teratomas consisting of all three germ layers after transplantation, later stage differentiation cultures tended to produce small size teratomas with ectodermal and mesodermal components. These small clusters were observed in recipient brains at 3 months posttransplantation, a time point when undifferentiated ES cells usually have produced large teratomas (5,16,44,45). It is unclear whether these donor cells would eventually develop into large teratomas, or cease proliferation. However, an analysis of expression patterns of proliferation, apoptosis,

and pluripotency markers suggest that small clusters differ from 3GL teratomas. The absence of SSEA1 and low PCNA signals further indicate that clusters are not comprised of stem/progenitor cells and will cease proliferation. The fact that small clusters only become visible upon close inspection of histological sections may indicate that they have been overseen in the past. In a few animals, the engrafted cells retained neural progenitor cell morphology or formed neural rosette-like structures. We interpret this as a sign of decreasing capacity for pluripotency consistent with the reduced in vitro colony formation. The neural predifferentiation of ES cells into pNPCs and the brain environment might have also biased the cellular composition of the donor towards ectodermal fate.

Together, we observed that AG ES cells exhibit neural developmental potential similar to that of N ES cells. Despite the unbalanced imprinting in AG ES-derived pNPCs and neural cells, neither their capacity to functional neurogenesis in vitro nor their tumorgenicity in vivo differ from N-derived cells. Due to the distinct features of uniparental cells that are related to their origin, our results indicate that AG neural stem cells can be used to study parent of origin-specific effects on neurogenesis.

ACKNOWLEDGMENTS: We thank Doris Heim and Barbara Gado for expert technical assistance in tissue processing, histology, and immunohistochemistry. This work was supported by the DFG-funded GRK 1048, the BMBF-funded Project 01GN0825, and the Interdisciplinary Center for Clinical Research (IZKF Würzburg), University Clinic of Würzburg (TP D103). The authors declare no conflicts of interest.

REFERENCES

1. Babak, T.; Deveale, B.; Armour, C.; Raymond, C.; Cleary, M. A.; van der Kooy, D.; Johnson, J. M.; Lim, L. P. Global survey of genomic imprinting by transcriptome sequencing. Curr. Biol. 18(22):1735–1741; 2008.
2. Barton, S. C.; Surani, M. A.; Norris, M. L. Role of paternal and maternal genomes in mouse development. Nature 311(5984):374–376; 1984.
3. Birger, Y.; Shemer, R.; Perk, J.; Razin, A. The imprinting box of the mouse Igf2r gene. Nature 397(6714):84–88; 1999.
4. Bock, C.; Reither, S.; Mikeska, T.; Paulsen, M.; Walter, J.; Lengauer, T. BiQ Analyzer: Visualization and quality control for DNA methylation data from bisulfite sequencing. Bioinformatics 21(21):4067–4068; 2005.
5. Brederlau, A.; Correia, A. S.; Anisimov, S. V.; Elmi, M.; Paul, G.; Roybon, L.; Morizane, A.; Bergquist, F.; Riebe, I.; Nannmark, U.; Carta, M.; Hanse, E.; Takahashi, J.; Sasai, Y.; Funa, K.; Brundin, P.; Eriksson, P. S.; Li, J. Y. Transplantation of human embryonic stem cell-derived cells to a rat model of Parkinson's disease: Effect of in vitro differentiation on graft survival and teratoma formation. Stem Cells 24(6):1433–1440; 2006.
6. Brustle, O.; Spiro, A. C.; Karram, K.; Choudhary, K.; Okabe, S.; McKay, R. D. In vitro-generated neural precursors participate in mammalian brain development. Proc. Natl. Acad. Sci. USA 94(26):14809–14814; 1997.
7. Buhnemann, C.; Scholz, A.; Bernreuther, C.; Malik, C. Y.; Braun, H.; Schachner, M.; Reymann, K. G.; Dihne, M. Neuronal differentiation of transplanted embryonic stem cell-derived precursors in stroke lesions of adult rats. Brain 129(Pt 12):3238–3248; 2006.
8. Capela, A.; Temple, S. LeX/ssea-1 is expressed by adult mouse CNS stem cells, identifying them as nonependymal. Neuron 35(5):865–875; 2002.
9. Choi, S. W.; Eckardt, S.; Ahmad, R.; Wolber, W.; McLaughlin, K. J.; Sirén, A. L.; Müller, A. M. Two paternal genomes are compatible with dopaminergic in vitro and in vivo differentiation. Int. J. Dev. Biol. 54:1755–1762; 2010.
10. Cibelli, J. B.; Grant, K. A.; Chapman, K. B.; Cunniff, K.; Worst, T.; Green, H. L.; Walker, S. J.; Gutin, P. H.; Vilner, L.; Tabar, V.; Dominko, T.; Kane, J.; Wettstein, P. J.; Lanza, R. P.; Studer, L.; Vrana, K. E.; West, M. D. Parthenogenetic stem cells in nonhuman primates. Science 295(5556):819; 2002.
11. Cui, L.; Johkura, K.; Yue, F.; Ogiwara, N.; Okouchi, Y.; Asanuma, K.; Sasaki, K. Spatial distribution and initial changes of SSEA-1 and other cell adhesion-related molecules on mouse embryonic stem cells before and during differentiation. J. Histochem. Cytochem. 52(11):1447–1457; 2004.
12. Damjanov, I.; Andrews, P. W. The terminology of teratocarcinomas and teratomas. Nat. Biotechnol. 25(11):1212; discussion 1212; 2007.
13. Davies, W.; Isles, A. R.; Wilkinson, L. S. Imprinted gene expression in the brain. Neurosci. Biobehav. Rev. 29(3):421–430; 2005.
14. De Miguel, M. P.; Fuentes-Julian, S.; Alcaina, Y. Pluripotent stem cells: Origin, maintenance and induction. Stem Cell Rev. 6(4):633–649; 2010.
15. DeVeale, B.; van der Kooy, D.; Babak, T. Critical evaluation of imprinted gene expression by RNA-Seq: A new perspective. PLoS Genet. 8(3):e1002600; 2012.
16. Dihne, M.; Bernreuther, C.; Hagel, C.; Wesche, K. O.; Schachner, M. Embryonic stem cell-derived neuronally committed precursor cells with reduced teratoma formation after transplantation into the lesioned adult mouse brain. Stem Cells 24(6):1458–1466; 2006.
17. Dinger, T. C.; Choi, S. W.; Eckardt, S.; McLaughlin, F.; Müller, A. M. Androgenetic embryonic stem cells form neural progenitor cells in vivo and in vitro. Stem Cells 26:1474–1483; 2008.
18. Dubois-Dauphin, M.; Julien, S. Stem cell-derived neurons grafted in the striatum are expelled out of the brain after chronic cortical stroke. Stroke 41(8):1807–1814; 2010.
19. Eckardt, S.; Dinger, T. C.; Kurosaka, S.; Leu, N. A.; Müller, A. M.; McLaughlin, K. J. Uniparental embryonic stem cells in development and transplantation. Organogenesis 4:1:33–41; 2008.
20. Eckardt, S.; Leu, N. A.; Bradley, H. L.; Bunting, K. D.; McLaughlin, K. J. Hematopoietic reconstitution with androgenetic and gynogenetic stem cells. Genes Dev. 21:409–419; 2007.
21. Ferrón, S. R.; Charalambous, M.; Radford, E.; McEwen, K.; Wildner, H.; Hind, E.; Morante-Redolat, J. M.; Laborda, J.; Guillemot, F.; Bauer, S. R.; Farinas, I.; Ferguson-Smith, A. C. Postnatal loss of Dlk1 imprinting in stem cells and niche astrocytes regulates neurogenesis. Nature 475(7356): 381–385; 2011.
22. Goldring, C. E.; Duffy, P. A.; Benvenisty, N.; Andrews, P. W.; Ben-David, U.; Eakins, R.; French, N.; Hanley, N. A.; Kelly,

L.; Kitteringham, N. R.; Kurth, J.; Ladenheim, D.; Laverty, H.; McBlane, J.; Narayanan, G.; Patel, S.; Reinhardt, J.; Rossi, A.; Sharpe, M.; Park, B. K. Assessing the safety of stem cell therapeutics. Cell Stem Cell 8(6):618–628; 2011.
23. Graham, C. F. The production of parthenogenetic mammalian embryos and their use in biological research. Biol. Rev. Camb. Philos. Soc. 49(3):399–424; 1974.
24. Gregg, C.; Zhang, J.; Weissbourd, B.; Luo, S.; Schroth, G. P.; Haig, D.; Dulac, C. High-resolution analysis of parent-of-origin allelic expression in the mouse brain. Science 329(5992):643–648; 2010.
25. Haupt, S.; Edenhofer, F.; Peitz, M.; Leinhaas, A.; Brustle, O. Stage-specific conditional mutagenesis in mouse embryonic stem cell-derived neural cells and postmitotic neurons by direct delivery of biologically active Cre recombinase. Stem Cells 25(1):181–188; 2007.
26. Hernandez, L.; Kozlov, S.; Piras, G.; Stewart, C. L. Paternal and maternal genomes confer opposite effects on proliferation, cell-cycle length, senescence, and tumor formation. Proc. Natl. Acad. Sci. USA 100(23):13344–13349; 2003.
27. Hiura, H.; Komiyama, J.; Shirai, M.; Obata, Y.; Ogawa, H.; Kono, T. DNA methylation imprints on the IG-DMR of the Dlk1-Gtl2 domain in mouse male germline. FEBS Lett. 581(7):1255–1260; 2007.
28. Isles, A. R.; Davies, W.; Wilkinson, L. S. Genomic imprinting and the social brain. Philos. Trans. R. Soc. Lond. B Biol. Sci. 361(1476):2229–2237; 2006.
29. Keverne, E. B. Genomic imprinting and the maternal brain. Prog. Brain Res. 133:279–285; 2001.
30. Kim, K.; Ng, K.; Rugg-Gunn, P. J.; Shieh, J. H.; Kirak, O.; Jaenisch, R.; Wakayama, T.; Moore, M. A.; Pedersen, R. A.; Daley, G. Q. Recombination signatures distinguish embryonic stem cells derived by parthenogenesis and somatic cell nuclear transfer. Cell. Stem Cell 1(3):346–352; 2007.
31. Koch, P.; Opitz, T.; Steinbeck, J. A.; Ladewig, J.; Brustle, O. A rosette-type, self-renewing human ES cell-derived neural stem cell with potential for in vitro instruction and synaptic integration. Proc. Natl. Acad. Sci. USA 106(9):3225–3230; 2009.
32. Kokaia, Z.; Martino, G.; Schwartz, M.; Lindvall, O. Cross-talk between neural stem cells and immune cells: The key to better brain repair? Nat.Neurosci. 15(8):1078–1087; 2012.
33. Kumamaru, H.; Ohkawa, Y.; Saiwai, H.; Yamada, H.; Kubota, K.; Kobayakawa, K.; Akashi, K.; Okano, H.; Iwamoto, Y.; Okada, S. Direct isolation and RNA-seq reveal environment-dependent properties of engrafted neural stem/progenitor cells. Nat. Commun. 3:1140; 2012.
34. Lendahl, U.; Zimmerman, L. B.; McKay, R. D. CNS stem cells express a new class of intermediate filament protein. Cell 60(4):585–595; 1990.
35. Lu, Z.; Zhu, W.; Yu, Y.; Jin, D.; Guan, Y.; Yao, R.; Zhang, Y. A.; Zhang, Y.; Zhou, Q. Derivation and long-term culture of human parthenogenetic embryonic stem cells using human foreskin feeders. J. Assist. Reprod. Genet. 27(6):285–291; 2010.
36. McGrath, J.; Solter, D. Completion of mouse embryogenesis requires both the maternal and paternal genomes. Cell 37(1):179–183; 1984.
37. Morali, O. G.; Jouneau, A.; McLaughlin, K. J.; Thiery, J. P.; Larue, L. IGF-II promotes mesoderm formation. Dev. Biol. 227(1):133–145; 2000.
38. Muotri, A. R.; Nakashima, K.; Toni, N.; Sandler, V. M.; Gage, F. H. Development of functional human embryonic stem cell-derived neurons in mouse brain. Proc. Natl. Acad. Sci. USA 102(51):18644–18648; 2005.
39. Neaves, W. B.; Baumann, P. Unisexual reproduction among vertebrates. Trends Genet. 27(3):81–88; 2011.
40. Okabe, S.; Forsberg-Nilsson, K.; Spiro, A. C.; Segal, M.; McKay, R. D. Development of neuronal precursor cells and functional postmitotic neurons from embryonic stem cells in vitro. Mech. Dev. 59(1):89–102; 1996.
41. Polentes, J.; Jendelova, P.; Cailleret, M.; Braun, H.; Romanyuk, N.; Tropel, P.; Brenot, M.; Itier, V.; Seminatore, C.; Baldauf, K.; Turnovcova, K.; Jirak, D.; Teletin, M.; Come, J.; Tournois, J.; Reymann, K.; Sykova, E.; Viville, S.; Onteniente, B. Human induced pluripotent stem cells improve stroke outcome and reduce secondary degeneration in the recipient brain. Cell Transplant. 21(12):2587–2602; 2012.
42. Raslan, F.; Albert-Weissenberger, C.; Ernestus, R. I.; Kleinschnitz, C.; Sirén, A. L. Focal brain trauma in the cryogenic lesion model in mice. Exp. Transl. Stroke Med. 4:6; 2012.
43. Revazova, E. S.; Turovets, N. A.; Kochetkova, O. D.; |Kindarova, L. B.; Kuzmichev, L. N.; Janus, J. D.; Pryzhkova, M. V. Patient-specific stem cell lines derived from human parthenogenetic blastocysts. Cloning Stem Cells 9(3):432–449; 2007.
44. Roy, N. S.; Cleren, C.; Singh, S. K.; Yang, L.; Beal, M. F.; Goldman, S. A. Functional engraftment of human ES cell-derived dopaminergic neurons enriched by coculture with telomerase-immortalized midbrain astrocytes. Nat. Med. 12(11):1259–1268; 2006.
45. Seminatore, C.; Polentes, J.; Ellman, D.; Kozubenko, N.; Itier, V.; Tine, S.; Tritschler, L.; Brenot, M.; Guidou, E.; Blondeau, J.; Lhuillier, M.; Bugi, A.; Aubry, L.; Jendelova, P.; Sykova, E.; Perrier, A. L.; Finsen, B.; Onteniente, B. The postischemic environment differentially impacts teratoma or tumor formation after transplantation of human embryonic stem cell-derived neural progenitors. Stroke 41(1):153–159; 2010.
46. Surani, M. A.; Barton, S. C.; Norris, M. L. Development of reconstituted mouse eggs suggests imprinting of the genome during gametogenesis. Nature 308(5959):548–550; 1984.
47. Surani, M. A.; Barton, S. C.; Norris, M. L. Nuclear transplantation in the mouse: Heritable differences between parental genomes after activation of the embryonic genome. Cell 45(1):127–136; 1986.
48. Takada, S.; Tevendale, M.; Baker, J.; Georgiades, P.; Campbell, E.; Freeman, T.; Johnson, M. H.; Paulsen, M.; Ferguson-Smith, A. C. Delta-like and gtl2 are reciprocally expressed, differentially methylated linked imprinted genes on mouse chromosome 12. Curr. Biol. 10(18):1135–1138; 2000.
49. Vierbuchen, T.; Ostermeier, A.; Pang, Z. P.; Kokubu, Y.; Sudhof, T. C.; Wernig, M. Direct conversion of fibroblasts to functional neurons by defined factors. Nature 463(7284):1035–1041; 2010.
50. Wang, X.; Sun, Q.; McGrath, S. D.; Mardis, E. R.; Soloway, P. D.; Clark, A. G. Transcriptome-wide identification of novel imprinted genes in neonatal mouse brain. PLoS One 3(12):e3839; 2008.
51. Wilkinson, L. S.; Davies, W.; Isles, A. R. Genomic imprinting effects on brain development and function. Nat. Rev. Neurosci. 8(11):832–843; 2007.